

Time-dependent growth of zinc hydroxide nanostrands and their crystal structure†

Xinsheng Peng,^{ab} Jian Jin,^a Noriko Kobayashi,^a Wolfgang Schmitt^c and Izumi Ichinose^{*a}

Received (in Cambridge, UK) 19th December 2007, Accepted 22nd January 2008

First published as an Advance Article on the web 18th February 2008

DOI: 10.1039/b719497h

Positively-charged crystalline zinc hydroxide nanostrands with a diameter of 2 nm and a length of a few micrometres rapidly grew in dilute aqueous solution of zinc nitrate and aminoethanol. The nanostrands were composed of hexagonal clusters of $[\text{Zn}_{61}(\text{OH})_{116}(\text{H}_2\text{O})_n]^{6+}$.

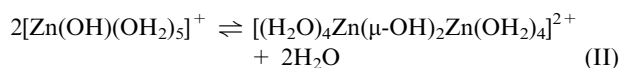
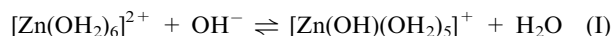
Inorganic nanofibres have been attracted increasing attention due to their great potential in various practical applications.¹ Among the preparation methods, synthesis in an aqueous system is considered as a promising route in terms of the large-scale production and the cost. A general approach to give rise to inorganic nanofibres in water is template synthesis, which has been widely studied in the past two decades.² The method also enabled us to produce inorganic sheets, tubes, and complicated hierarchal structures.³ On the other hand, in some reports, nanomorphologies of inorganic materials were controlled without using a template.⁴ For example, Kotov and his co-workers reported spontaneous conversion of CdTe nanoparticles into nanowires through an orientation attachment mechanism.⁵ It is well known that nanofibres of vanadium oxide spontaneously form in water by the polycondensation of vanadic acid.⁶ Nanofibres of copper hydroxide are similarly obtained.⁷ Synthesis in aqueous solution is also favorable for the reduction of harmful substances.

We reported that cadmium and copper hydroxide nanostrands were formed by simply raising the pH of the aqueous solutions of the corresponding metal nitrates.⁸ They are highly positively charged and strongly adsorb negatively charged DNA and proteins.⁸ Such nanostrands have been widely used as components of various nanocomposites and nanofibrous membranes.⁸ The simplicity of the synthetic procedure enhances their appeal for many industrial applications. However, the big disadvantage of these materials (in particular of the cadmium hydroxide nanostrand) is their toxicity. In order to overcome this toxicological limitation, we have thoroughly investigated the formation of the nanostrands of commonly used materials.

Herein, we report the discovery of zinc hydroxide nanostrands. Zinc hydroxide is a layered material, and in general, it precipitates from a zinc salt solution, when the pH of the solution is raised.⁹ However, we observed a wide morphological diversity at the beginning of the formation process, and extremely long and thin structures were temporarily found in certain pH and concentration conditions. This is the first report of one-dimensional nanostructures of zinc hydroxide that have long been produced in industry as a precursor of zinc oxide and for the applications such as surgical dressings, separation of proteins, *etc.*¹⁰

Zinc hydroxide nanostrands were prepared by mixing 5 mL of aqueous aminoethanol (AE, 2.4 mM) into an equivolume of zinc nitrate solution (4 mM) by using a magnetic stirrer. The resulting solution (AE/Zn = 0.6) kept transparent for a while. However, despite this transparency, abundant nanostrands formed in the solution. The nanostrands were filtered off after an aging time of 30 min. SEM image revealed that the length of these nanostrands reached a few micrometres (Fig. 1). The morphologies of zinc hydroxide were strongly dependent on the conditions. The results are described in detail in the ESI.†

When the amount of aminoethanol is less than half of that necessary for the stoichiometric precipitation of $\text{Zn}(\text{OH})_2$, a water molecule coordinating to a hydrated zinc ion is replaced with a hydroxide ion (eqn (I)). Then, the hydroxide ion bridges to another zinc ion through ololation, for example, giving a dinuclear complex (eqn (II)).



In reality, the ololation process is not so simple, and various multinuclear complexes form. Our isolated zinc hydroxide

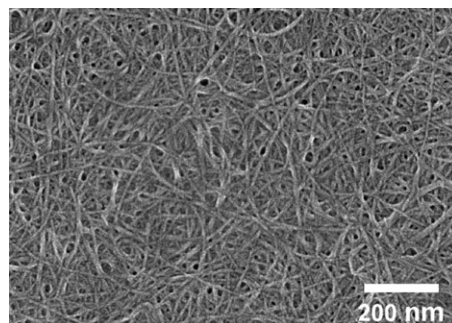


Fig. 1 SEM image of zinc hydroxide nanostrands.

^a Organic Nanomaterials Center (ONC), National Institute for Materials Science (NIMS), 1-1 Namiki, Tsukuba, Ibaraki 305-0044, Japan. E-mail: ICHINOSE.Izumi@nims.go.jp; Fax: +81-29-852-7449

^b International Center for Young Scientists (ICYS), NIMS, Japan

^c University of Dublin, Trinity College, School of Chemistry, Dublin 2, Ireland

† Electronic supplementary information (ESI) available: Experimental details, nanomorphologies of zinc hydroxide, formation of bundles, EDX measurements, estimation of positive charges, and comparison of metal hydroxide nanostrands. See DOI: 10.1039/b719497h

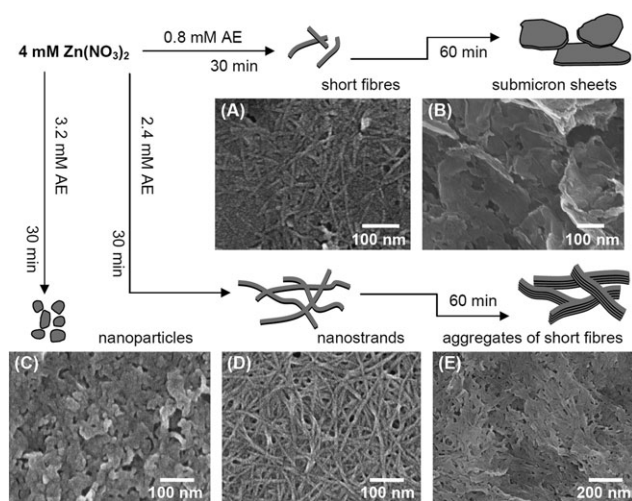


Fig. 2 Morphology changes of zinc hydroxide at different concentrations of aminoethanol (AE) and typical SEM images. (A) 0.8 mM AE, after 30 min aging, (B) 0.8 mM AE, after 1 h aging, (C) 3.2 mM AE, after 30 min aging, (D) 2.4 mM AE, after 30 min aging, and (E) 2.4 mM AE, after 1 h aging.

nanostrands can be seen as one type of nanomorphology that results from condensation of hydroxo-bridged clusters produced by a small amount of aminoethanol.

Our systematic investigation revealed that the nanomorphology changes with the concentration of zinc nitrate, the molar ratio of aminoethanol, and especially with the aging time of the mixed solution. Fig. 2 shows SEM images of representative morphologies. When an aqueous solution of 4 mM zinc nitrate was mixed with an equivalent volume of 0.8 mM aminoethanol, short fibres were initially obtained (Fig. 2A). However, these fibres were consequently converted into submicron sheets after 60 min of aging (Fig. 2B). When the concentration of aminoethanol was increased to 3.2 mM, nanoparticles of a few tens of nanometres formed (Fig. 2C), and precipitated from the solution. Long and thin nanostrands were obtained from 4 mM zinc nitrate and 2.4 mM aminoethanol solutions after an aging time of 30 min (Fig. 2D). However, these nanostrands converted into the aggregates of short fibres after 60 min aging (Fig. 2E). We have not succeeded in the preparation of zinc hydroxide nanostrands using sodium hydroxide (see ESI[†]); a weak organic base seems to be indispensable. The surfaces of nanostrand are probably coordinated in part by aminoethanol, which seems to stabilise the one-dimensional structure of zinc hydroxide. Nanostrands were also produced from 6 mM $\text{Zn}(\text{NO}_3)_2$ and 2.4 mM aminoethanol solutions after 30 min aging. However, the nanostrands formed under these conditions were unstable and started to precipitate when the solution was left for a further 10 min.

Adsorption experiments of a negatively charged dye molecule, Evans Blue, were conducted to estimate the surface charges of zinc hydroxide nanostrand. This dye molecule strongly adsorbed on the nanostrands and gave weakly-gelled precipitates. In contrast, such precipitation was not observed in corresponding systems that contained only hydrated zinc ions. After a certain volume of the nanostrand solution was mixed with an Evans Blue solution, the blue precipitates formed were filtered off. The

color changes in filtrates were monitored by using UV-vis absorption spectroscopy, increasing the volume of the nanostrand solution (see ESI[†]). From the spectra, we estimated that at least one hundred and twenty five zinc atoms were necessary to remove one Evans Blue molecule from the solution. In our experiments, the conversion ratio of zinc atoms to the nanostrands is *ca.* 30% and one Evans Blue molecule has four sulfonate groups. Considering these preconditions, about one tenth of the zinc atoms in the nanostrand seem to be positively charged. We also verified the amount of positively charged zinc atoms by energy dispersive X-ray (EDX) measurements (see ESI[†]). The spectra obtained for the blue precipitates gave the atomic ratio of 30 : 3 for zinc : sulfur, indicating that about 10% of the zinc atoms were positively charged.

Fig. 3A and 3B shows DF-STEM (dark field scanning transmission electron microscopy) images. This method provides a significant atomic-number-dependent contrast. The nanostrands in these images have a width of 2.0 ± 0.2 nm and appear to be isolated from each other. After an aging time of 45 min, the bundle-like structures were observed (see ESI[†]). This indicates that the nanostrands tend to aggregate with increasing aging time. The zinc hydroxide nanostrand is a crystalline material. SAED (selected area electron diffraction) measurements revealed that its crystallographic structure is consistent with that of hexagonal β -zinc hydroxide.¹¹ The diffraction pattern shown in Fig. 3A was assigned to the (100), (002), (102) and (110) planes. The EDX spectra of these nanostrands showed the atomic ratio of 32 : 68 for zinc and oxygen atoms, which was in good agreement with the composition of zinc hydroxide. Fig. 3C shows a high-resolution TEM image of zinc hydroxide nanostrands. One of the enlarged images is shown in Fig. 3D. The lattice spacing of 0.235 nm corresponds to the (002) planes of β -zinc hydroxide.¹¹ This means that the nanostrand grew along the (001) direction. The crystal lattice seems to be continuous along the nanostrand. The image shown in Fig. 3D displays a representative zigzag structure often observed in our sample. The bent angles in the structure are 119.3 degrees. The angle between the axis of nanostrand and the (002) plane is 29.3 degrees. The atomic lattice structure revealed that the cross-section of the nanostrand is composed of nine atoms with an overall width of 2.21_2 nm (marked by the circles in Fig. 3D). Consequently, the width of the nanostrand was calculated to be 1.93 nm, considering the width (2.21_2 nm) parallel to the (002) plane and the cosine of 29.3 degrees.

The crystal structure model obtained using a crystal structure analysis software (ATMOS V6.12) is shown in Fig. 3E. The calculations are based on the trigonal $P\bar{3}m1$ space group of β -zinc hydroxide and the lattice parameters of $a = b = 3.192$ Å and $c = 4.65$ Å. From the width of 2.21_2 nm, we propose a hexagonal plate consisting of sixty-one zinc atoms as the basic building unit of the nanostrand. This unit contains nine zinc atoms along the $\langle -110 \rangle$ line, which is in agreement with the TEM observation. Six atoms at the corners are supposed to be positively charged. This assignment is supported by the adsorption experiments of Evans Blue and EDX measurements that demonstrate one tenth of the zinc atoms are positively charged, where the formula is described as $[\text{Zn}_{61}(\text{OH})_{116}(\text{H}_2\text{O})_n]^{6+}$. The high-resolution TEM image was accurately replicated by assembling such hexagonal plates along the c -axis, keeping the

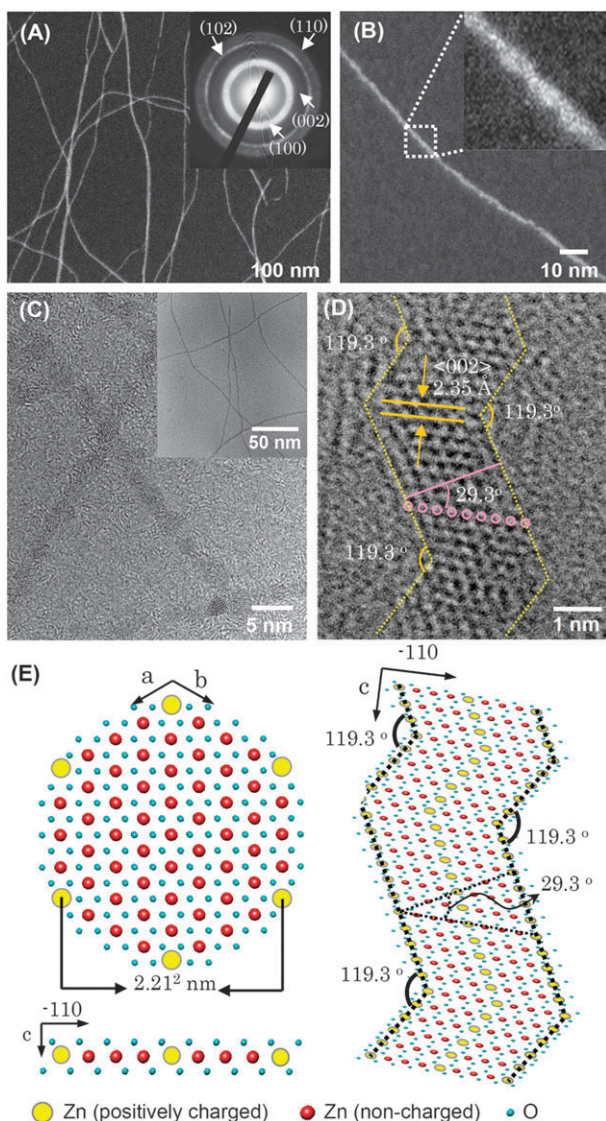


Fig. 3 Dark field STEM (A, B) and HR-TEM (C, D) images of zinc hydroxide nanostrands and the crystal structure (E). The inserts in (A) and (C) are the corresponding SAED pattern and low-magnification TEM image. Hydrogen atoms are not shown in (E).

crystallographic structure of β -zinc hydroxide. It should be emphasized that the individual hexagonal plates with positively charged corners interact with each other through strong multiple hydrogen bonding. This results in the crystal growth along the c -axis, preventing the growth in the directions of the a - and b -axes. The zigzag structure is also reproducible by shifting the hexagonal plates in the directions parallel to the (001) plane. This shifting seems to be important to relieve the electrostatic repulsion between positively charged zinc atoms.

The zinc hydroxide nanostrands formed after 30 min aging always begin to aggregate with further aging. The stability in solution is no more than one hour, which is much shorter than that of cadmium hydroxide nanostrands (1 day) and copper hydroxide nanostrands (1 month). The DLVO theory explains that the stability of colloidal particles is governed by the electrostatic repulsion and the van der Waals attraction.¹² The theory has been applied for the dispersion of charged

nanoparticles in water.¹³ In the cases of the above three nanostrands, the concentration of the metal ions, the pH of the solutions, and the diameter of the nanostrands are very close. The difference results from the surface charge density. As shown in Fig. 3E, one quarter of the surface zinc atoms in the nanostrand are positively charged. In contrast, one-third of the surface atoms of the cadmium hydroxide nanostrand and half of the surface atoms of the copper hydroxide nanostrand are positively charged (see ESI[†]). The high charge density is needed to prevent the nanostrands from aggregation and to give the nanostrands stability in water. However, the high aspect ratio of zinc hydroxide nanostrands successfully allows a facile separation from the solution by filtration.

In conclusion, we report the discovery of positively charged crystalline zinc hydroxide nanostrands, which are composed of hexagonal $[\text{Zn}_{61}(\text{OH})_{116}(\text{H}_2\text{O})_n]^{6+}$ clusters. This polymer-like inorganic material was temporarily formed in water. But, they are stable in air and in vacuum, if isolated from the solution. It is notable that zinc is an essential element for human beings. The recommended intake for an adult man is said to be *ca.* 10 mg per day. This is in strong contrast to the high toxicity of cadmium ions. Such safety considerations become imperative when nanomaterials are widely used in industry. This nanostrand instantly dissolves in acidic solution and is expected to be less hazardous than stable nanomaterials such as carbon nanotubes. Furthermore, the rapid growth of zinc hydroxide nanostrands allows the design of continuous production processes in flow reactors.

Notes and references

- 1 Y. Xia, P. Yang, Y. Sun, Y. Wu, B. Mayers, B. Gates, Y. Yin, F. Kim and H. Yan, *Adv. Mater.*, 2003, **15**, 353.
- 2 (a) S. Mann, *Chem. Commun.*, 2004, 1; (b) L. A. Estroff and A. D. Hamilton, *Chem. Mater.*, 2001, **13**, 3227.
- 3 (a) J. D. Hartgerink, E. Beniash and S. I. Stupp, *Science*, 2001, **294**, 1684; (b) S.-H. Yu, M. Antonietti, H. Cölfen and J. Hartmann, *Nano Lett.*, 2003, **3**, 379.
- 4 (a) M. Niederberger and H. Cölfen, *Phys. Chem. Chem. Phys.*, 2006, **8**, 3271; (b) X. Zhong and W. Knoll, *Chem. Commun.*, 2005, 1158; (c) C. Lu, L. Qi, J. Yang, Li. Tang, D. Zhang and J. Ma, *Chem. Commun.*, 2006, 3551.
- 5 Z. Tang, N. A. Kotov and M. Giersig, *Science*, 2002, **297**, 237.
- 6 (a) J. Livage, *Coord. Chem. Rev.*, 1998, **178–180**, 999; (b) J. Muster, G. T. Kim, V. Krstić, J. G. Park, Y. W. Park, S. Roth and M. Burghard, *Adv. Mater.*, 2000, **12**, 420.
- 7 (a) Z. L. Wang, X. Y. Kong, X. Wen and S. J. Yang, *Phys. Chem. B*, 2003, **107**, 8275; (b) C. Lu, L. Qi, J. Yang, D. Zhang, N. Wu and J. Ma, *J. Phys. Chem. B*, 2004, **108**, 17825.
- 8 (a) I. Ichinose, K. Kurashima and T. Kunitake, *J. Am. Chem. Soc.*, 2004, **126**, 7162; (b) Y.-H. Luo, J. Huang, J. Jin, X. Peng, W. Schmitt and I. Ichinose, *Chem. Mater.*, 2006, **18**, 1795; (c) I. Ichinose, J. Huang and Y.-H. Luo, *Nano Lett.*, 2005, **5**, 97; (d) Y.-H. Luo, J. Huang and I. Ichinose, *J. Am. Chem. Soc.*, 2005, **127**, 8296; (e) X. Peng, J. Jin, E. M. Ericsson and I. Ichinose, *J. Am. Chem. Soc.*, 2007, **129**, 8625; (f) X. Peng, J. Jin and I. Ichinose, *Adv. Funct. Mater.*, 2007, **17**, 1849.
- 9 R. A. McBride, J. M. Kelly and D. E. McCormack, *J. Mater. Chem.*, 2003, **13**, 1196.
- 10 (a) A. N. Eryomin, M. V. Makarenko and L. P. Budnikova, *Appl. Biochem. & Microbiol.*, 2005, **41**, 336; (b) T. V. Letonoff, *J. Biol. Chem.*, 1934, **106**, 693; (c) R. Burcelin, W. Dolci and B. Thorens, *Diabetes*, 2000, **49**, 1635.
- 11 Powder Diffraction File, 24-1444.
- 12 J. N. Israelachvili, *Intermolecular and Surface Forces*, Academic Press, London, 2nd edn., 1992.
- 13 (a) T. Kim, K. Lee, M.-S. Gong and S.-W. Joo, *Langmuir*, 2005, **21**, 9524; (b) K. L. Chen and M. Elimelech, *Langmuir*, 2006, **22**, 10994.